

Impact of Power Factor Control Loop at Rectifier Unit on Wind Turbine Driven Self-Excited Induction Generator Connected to Grid

Swati Devabhaktuni and S. V. Jayaram Kumar

Abstract—This paper presents an effect of power factor control loop at rectifier unit, placed in between, Self excited induction generator and grid along with the inverter. The power factor control scheme does not require any system parameters, such as the values of the line inductance or filter capacitor. Variations in the line inductance due to the power system operation or the changes in filter capacitor size do not affect the process of tracking unity or maximum power factor. The main objective of this paper is to track the maximum power of the grid connected SEIG driven by wind turbine and to reduce the ripples in power factor, active and reactive power at the grid. In previous literature there is no discussion about the improvement and reduction of ripples in the power factor at the grid. The variable magnitude, variable frequency, voltage of the generator can be controlled by the proper modulation index. By controlling both modulation index and delay angle simultaneously, the rectifier can potentially achieve unity power factor operation while its dc current can also be controlled. The results are valid through MATLAB/SIMULINK software.

Index Terms—Self Excited Induction Generator (SEIG), Wind turbine, Hybrid nine level inverter, Voltage source rectifier, Grid, Power factor loop.

I. INTRODUCTION

It is well known that a three-phase induction machine can be made to work as a self-excited induction generator. When capacitors are connected across the stator terminals of an induction machine, driven by an external prime mover, voltage will be induced at its terminals. In a small wind power plant or hydro power plant, the use of a three-phase self-excited induction generator (SEIG) is essential. An SEIG provides capacitor banks to compensate for the power factor, and the active power controller and the reactive power controller are coupled, unlike a synchronous machine. This means that the control of an SEIG is complex; an SEIG can be damaged by overvoltage due to capacitors [1].

The cage-type induction generators have emerged in these recent years as a suitable candidate in remote areas where this machine can be driven using a wind turbine, a diesel engine or small hydro plants [6]. Normally, in this last application, the SEIG generates constant voltage and frequency because it is operating at constant load power.

In remote areas the devoid of supply will be electrified by utilizing the renewable energy resources such as wind, solar,

biomass, hydro *etc.* The most suitable power generation for such remote areas will be operated with self excited induction generator due to its simplicity, robust, cheap, reliable, ruggedness, overload protection, absence of dc, little maintenance *etc.* It also has the self protection feature against overload [5], and does not require a DC exciter like synchronous generator [2]. However, poor voltage regulation is a great disadvantage of self-excited induction generators. Therefore, a control system is required to regulate the voltage to meet the constant voltage demand.

Nowadays wind energy shares substantial part of energy produced by non conventional energy sources. Researchers used self-excited induction generators in contrast to grid-connected induction generators in wind energy conversion systems due to their capability to generate power for a wide range of operating speeds [8].

In the SEIG, the excitation current is supplied by the capacitors connected across its terminals. The terminal voltage is regulated against changing the speed and load conditions, by changing the terminal capacitance and the variation of the frequency depends on the operating speed range [3]. The application of power semi conductor devices, and controlled converter circuits has resulted in suitable regulating schemes for self excited squirrel cage generators [4]. The above papers did not mention about the reduction of ripples in active power, reactive power and power factor at grid [7]. This paper exploits the possible ways to reduce the ripples at the grid and the power factor control scheme design such that at rectifier unit that the rectifier will (a) operate at a unity power factor when it is achievable and (b) produce the highest possible power factor when the unity power factor operation is not achievable.

The system we tested has the following components:

- a wind turbine;
- a three-phase, 3-hp, squirrel cage induction generator driven by the wind turbine;
- various sets of capacitors to provide reactive power to the induction generator;
- a three-phase diode bridge to rectify the current provided by the generator;
- a power factor loop;
- a shunt capacitor to smooth the dc voltage ripples;
- a three-phase Hybrid nine level inverter to convert the power from the dc bus to the utility.

II. PROPOSED SYSTEM

In the proposed system, a power generation system consisting of a wind turbine with SEIG connected to the grid through a power electronic converter and a power factor loop

Manuscript received September 5, 2011, revised November 11, 2011.

Swati Devabhaktuni is with the Department of electrical and electronic engineering, Gokaraju Rangaraju college of engineering, Hyderabad, India (e-mail:swatikjm@gmail.com).

S.V.Jayaram kumar is the professor, J. N. T. University, Hyderabad, India (e-mail:svjkumar101@rediffmail.com).

at the rectifier unit is considered. A proposed impedance source inverter based wind driven SEIG fed to grid is shown in Fig.1.

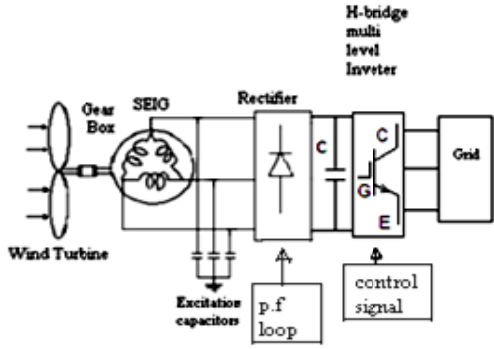


Fig. 1. Proposed SEIG model connected to grid.

The capacitor size can be reduced, when the Current Source Rectifier (CSR) operates at higher switching frequencies or the dual-bridge rectifier is used. Neglecting a small voltage drop across the line inductance, the capacitor voltage is approximately equal to the supply voltage, resulting in a constant current flowing through the capacitor regardless of the operating condition of the rectifier. The rectifier dc output current can be controlled by modulation index m_a . Alternatively, it can also be adjusted by delay angle, α in the same manner as that for phase-controlled SCR rectifiers. The delay angle, α control produces a lagging power factor, which compensates the leading power factor caused by the filter capacitor. By controlling both modulation index and delay angle simultaneously, the rectifier can potentially achieve unity power factor operation while its dc current can also be controlled. This proposed scheme is used to improve the power factor and reduce harmonic current. The parameters used in the SEIG can be obtained by conducting no load test and short circuit test on the induction generator when it is used as an induction motor. The traditional tests used to determine the parameters are the open circuit test and the short circuit test. The induction machine used as the SEIG in this investigation is a three-phase wound rotor induction motor with specification: 415V, 7.5A, 3kW, 50Hz, and 4 poles.

A. Characteristics of Wind Turbine

The wind turbine is characterized by the power coefficient C_p , which has no units, as a function of both the tip speed ratio, λ and the blade pitch angle, β . In order to fully utilize the available wind energy, the value of λ should be maintained at its optimum value. Therefore, the power coefficient corresponding to that value will become maximum also. The tip speed ratio λ can be defined as the ratio of the angular rotor speed of the wind turbine to the linear wind speed at the tip of the blades. It can be expressed as follows:

$$\lambda = \omega_r R / V_w \tag{1}$$

where R is the wind turbine rotor radius, V_w is the wind speed and ω_r is the mechanical angular rotor speed of the wind turbine.

The output power of the wind turbine, can be calculated from the following equation:

$$P_m = \frac{1}{2} \rho A C_p V_w^3 \tag{2}$$

where (ρ) is the air density, and (A) is the swept area by the

blades, and

$$C_p = (0.44 - 0.167\beta) \sin \left[\frac{\pi(\lambda - 3)}{15 - 0.3\beta} \right] - 0.00184(\lambda - 3)\beta \tag{3}$$

Also, the torque available from the wind turbine can be expressed as:

$$T_m = \frac{1}{2} \rho A C_T V_w^2 \tag{4}$$

where C_T is the torque coefficient which is given by

$$C_T = C_p / \lambda \tag{5}$$

Then, the aerodynamic torque, T_m can be written as follows:

$$T_m = 0.5 \rho A \left[(0.44 - 0.167\beta) \sin \left[\frac{\pi(\lambda - 3)}{15 - 0.3\beta} \right] - 0.00184(\lambda - 3)\beta \right] \frac{V_w^3}{\omega_t} \tag{6}$$

B. Self-excited Induction Generator

The induction machine is modeled using the steady-state equivalent circuit shown in Fig. 2.

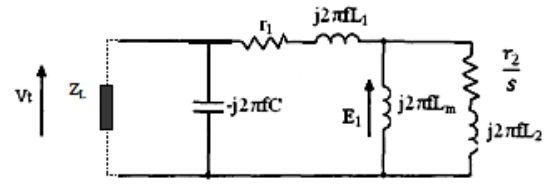


Fig. 2. Equivalent circuit of SEIG.

Flux linkages per second with saturation effect

$$\psi_{qs} = \omega_b \int \left[v_{qs} + \frac{r_s}{x_{ls}} (\psi_{mq}^{sat} - \psi_{qs}) \right] dt \tag{7}$$

$$\psi_{ds} = \omega_b \int \left[v_{ds} + \frac{r_s}{x_{ls}} (\psi_{md}^{sat} - \psi_{ds}) \right] dt \tag{8}$$

$$\psi'_{qr} = \omega_b \int \left[\frac{\omega_r}{\omega_b} \psi'_{dr} + \frac{r'_r}{x_{lr}} (\psi_{mq}^{sat} - \psi'_{qr}) \right] dt \tag{9}$$

$$\psi'_{dr} = \omega_b \int \left[-\frac{\omega_r}{\omega_b} \psi'_{qr} + \frac{r'_r}{x_{lr}} (\psi_{md}^{sat} - \psi'_{dr}) \right] dt \tag{10}$$

The stator qd0 currents can be calculated as:

$$i_{qs} = \frac{\psi_{qs} - \psi_{mq}^{sat}}{x_{ls}} \tag{11}$$

$$i_{ds} = \frac{\psi_{ds} - \psi_{md}^{sat}}{x_{ls}} \tag{12}$$

$$i_{0s} = \frac{\psi_{0s}}{x_{ls}} = \frac{\omega_b}{x_{ls}} \int (v_{0s} - r_s i_{0s}) dt \tag{13}$$

The electromagnetic torque equation is

$$T_{em} = \frac{3}{2} \frac{P}{2\omega_b} (\psi_{ds} i_{qs} - \psi_{qs} i_{ds}) \tag{14}$$

The model of self excited induction generator is implemented with simulink. It is divided in blocks that consider the transformations: abc-qd0 of the stator voltages and qd0-abc of the stator currents equations. The SEIG model is as shown in Fig. 3.

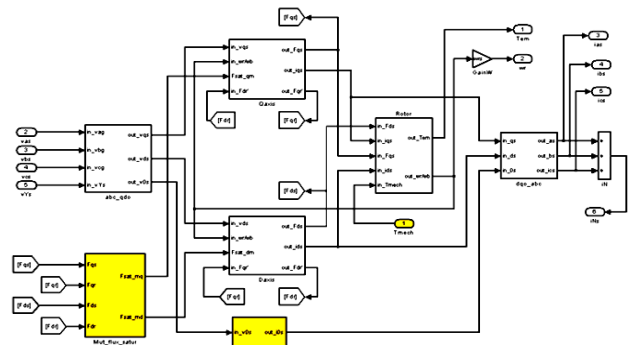


Fig. 3. Self excited induction generator model implemented in simulink.

The excitation capacitance required and frequency of the SEIG can be calculated from the equations

$$A_4 f^4 + A_3 f^3 + A_2 f^2 + A_1 f^1 + A_0 = 0 \quad (15)$$

$$C = \frac{af+b}{cf^3+df^2+e} \quad (16)$$

The constants are as given in APPENDIX.

C. Electronic Power Factor Control Loop Model

Three phase uncontrolled bridge rectifier is used to convert the variable voltage, variable frequency at the induction generator terminal into rectified dc voltage [3]. To simplify the analysis, all the diodes are assumed to be ideal (no power losses or on-state voltage drop).

The dc voltage V_d contains six pulses (humps) per cycle of the supply frequency. The rectifier is, therefore, commonly known as a six-pulse rectifier.

The average value of the dc voltage can be calculated by

$$V_d = \left[\frac{3\sqrt{2}}{\pi} \right] \left[\frac{\sqrt{3}}{\sqrt{2}} \right] \times V_{dc} \times \eta_i \quad (17)$$

The PWM current is in phase with the supply voltage V_s while the line current I_s leads V_s by the power factor angle. The input power factor of the rectifier is then given by

$$PF = DF \times \cos\Phi = \cos\Phi \quad (18)$$

where the distortion power factor DF is assumed to be unity, which is based on the fact that the waveform of the line current is close to sinusoidal. Under this assumption, the control of the power factor is essential to control the displacement power factor of the rectifier. The input power factor can be improved by increasing the delay angle α between PWM current I_w and V_s and in the meanwhile increasing the modulation index m_a to compensate the dc voltage reduction due to the increase of α . The dc voltage is a function of m_a and α , given by

$$V_d = \frac{\sqrt{3}}{2} V_{LL} m_a \cos\alpha \quad (19)$$

To achieve a unity power factor operation, the delay angle should satisfy

$$\alpha \approx \sin^{-1} \frac{I_c}{I_w} \approx \sin^{-1} \frac{\omega C f V_s}{m_a I_d} \quad (20)$$

Here the voltage drop on the line inductance is neglected.

A power factor control scheme presented in this paper is as shown in Fig.4.

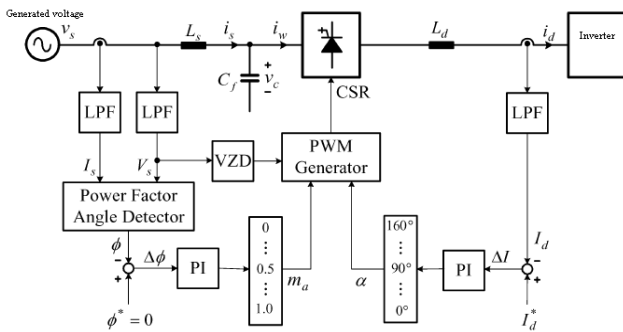


Fig. 4. Block diagram of power factor control scheme.

There exist two control loops. In the m_a control loop, the generated voltage V_s and line current I_s are detected through a low-pass filter (LPF) and then sent to the power factor angle detector. The detected power factor angle is compared with its reference Φ^* , which is normally set to zero, demanding a unity power factor operation. The resultant error signal $\Delta\Phi$ is used to control modulation index m_a through a PI regulator. In the α control loop, the detected dc current I_d is compared

with its reference I_d^* . The error signal ΔI is then sent to a PI for delay angle control. The dc current is essentially controlled by both m_a and α . The PWM generator produces the gate signals for the GCTs in the CSR based on calculated modulation index m_a and delay angle α . The voltage zero crossing detector (VZD) provides a reference for the delay angle control. The control scheme can guarantee that the input power factor of the rectifier is unity when it is achievable. Assuming that the line current I_s leads the supply voltage V_s by an angle due to a change in load, an error signal $\Delta\Phi$ is generated. This error signal results in a higher modulation index m_a , which boosts the dc voltage V_d . The increase in V_d makes the dc current I_d rise, which causes the α control loop to respond. The control loop tries to bring I_d back to the value set by I_d^* by increasing α . The increase in α causes a reduction in Φ , which improves the input power factor. This process continues until the unity power factor is reached, at which the power factor angle Φ equals zero, the phase displacement error $\Delta\Phi$ equals zero, the dc current I_d equals I_d^* , and the rectifier operates at a new operating point.

When the rectifier operates under light load conditions, the unity power factor operation may not be achievable. Similar to the case discussed above, the modulation index m_a keeps increasing due to $\Delta\Phi$, and in the meantime the delay angle α also keeps increasing for the dc current adjustment and power factor improvement.

Since $\Delta\Phi$ will not be reduced to zero, the process continues until the PI regulator in the m_a loop is saturated, at which m_a reaches its maximum value $m_{a,max}$ and the delay angle α also reaches a value that produces the highest possible input power factor while maintains I_d at its reference value. Obviously, the transition between the two operation modes, the unity and maximum power factor operations, is smooth and seamless. No extra measures should be taken for the transition.

It is worth noting that the power factor control scheme does not require any system parameters, such as the values of the line inductance or filter capacitor. Variations in the line inductance due to the power system operation or the changes in filter capacitor size do not affect the process of tracking unity or maximum power factor, which is desirable in practice.

D. Multi Level Inverters

The diode clamped multi level inverters are used to eliminate over voltage stress and reduce the switching frequency. By increasing the voltage levels of the inverter reduces the switching losses. To connecting the switching devices in parallel connections it leads to higher current levels. Multilevel inverter topologies are based on this principle, and therefore the voltages applied to the devices can be controlled and limited. Then number of H bridges is formed as 4. The no of bridges is equivalent to $\frac{m-1}{2}$ where n is the no of levels (here 9)[6] and the no of carrier waves for PWM control is equal to (m-1) overall for the positive and negative gate pulse generators. The range of the modulation index of the inverter is $0 \leq m \leq \frac{2}{\sqrt{3}}$. The number of output phase voltage levels is $M = \frac{N-1}{2}$.

The total number of active switches (IGBTs) used in the CHB inverters can be calculated by $N_{sw} = 6(m - 1)$.

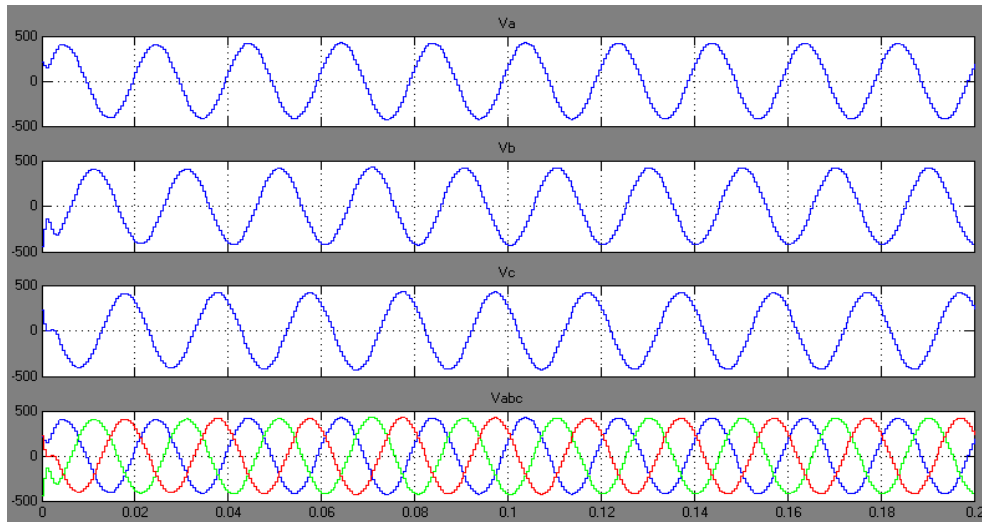


Fig. 6. SEIG generated voltages

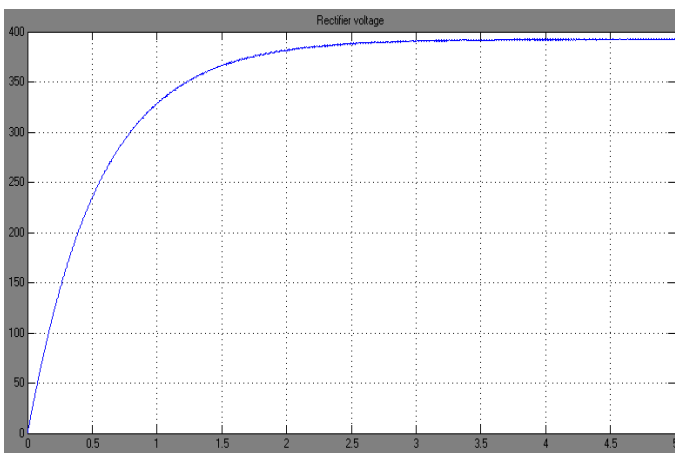


Fig. 7. Rectifier voltage.

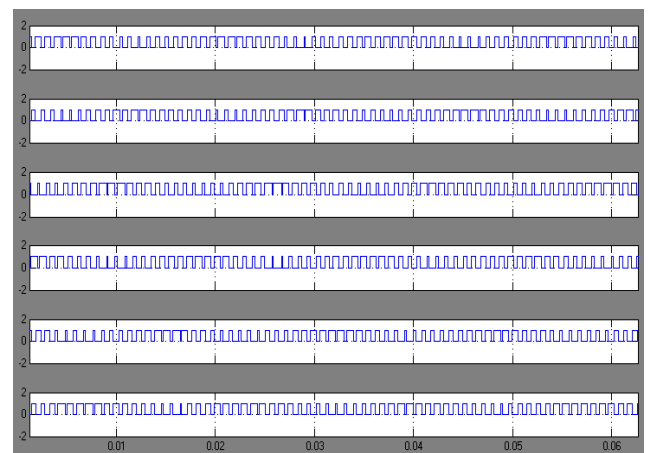


Fig. 10. Gate pulses at rectifier unit.

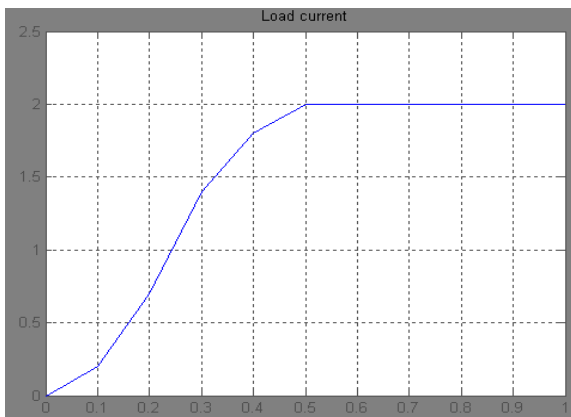


Fig. 8. Output current at rectifier.

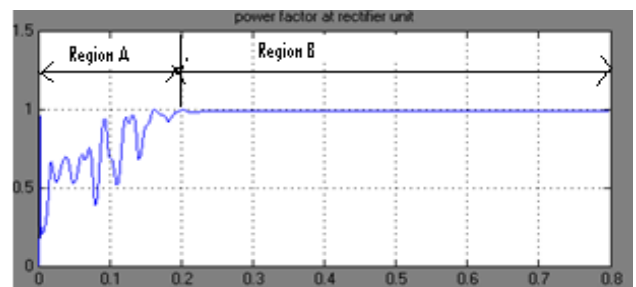


Fig. 11. Rectifier power factor.

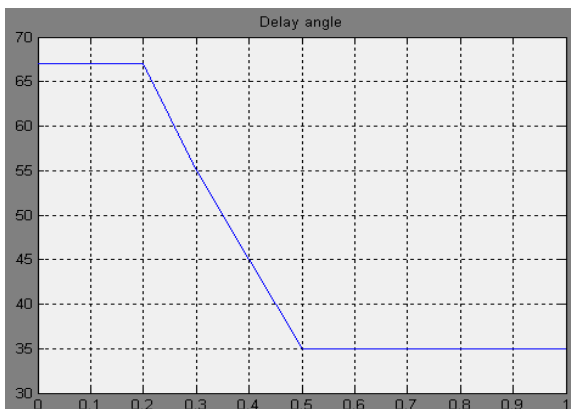


Fig. 9. Delay angle at power factor loop.

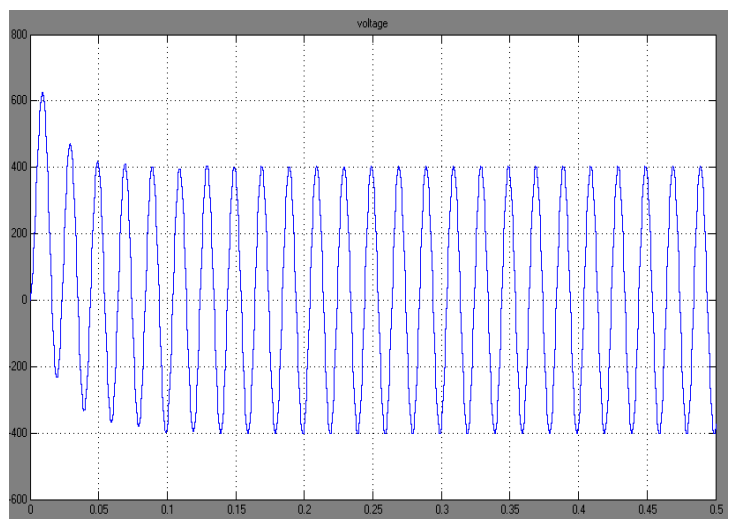


Fig. 12. Supply voltage to rectifier.

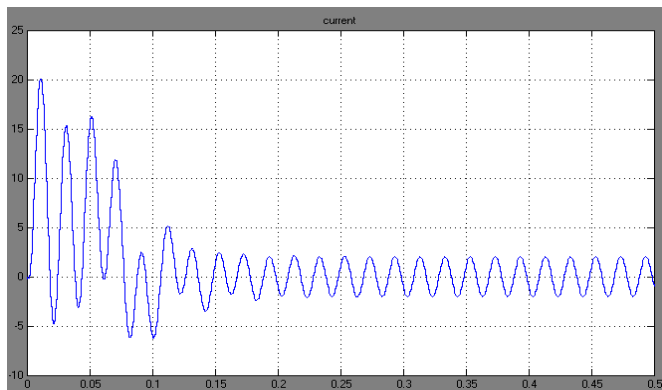


Fig. 13. Line current to rectifier.

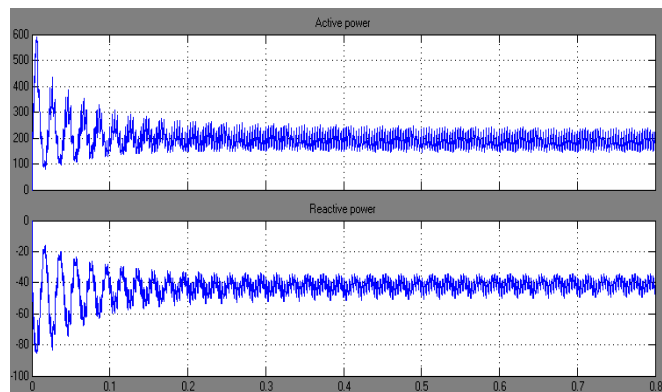


Fig. 14. Active and reactive power received by grid without control loop.

The power factor at the grid without power factor loop is as shown in Fig. 15. The p.f is varying between 0.7 to 0.8. The p.f reaches to steady state at 0.2 seconds. As reactive power is decreased and having a constant active power the p.f at the grid is increased. The p.f at the grid is of more harmonics in it.

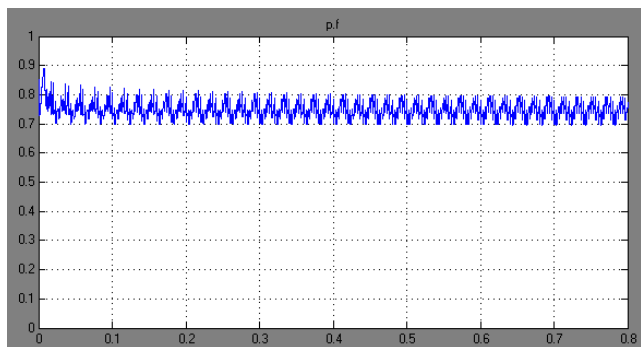


Fig. 15. Power factor at the grid without control loop.

The variation of p.f is also having more harmonics. These harmonics can be reduced with the power factor control loop used at the rectifier unit. The active power, reactive power and power factor variation is as shown in Fig. 16 & 17. With the use of this control loop there is no variation in the magnitude of the active power whereas there is a change in the reactive power and power factor. The advantage of using the power factor loop is, there is reduction in the harmonics of active power, reactive power and power factor at the grid. By varying the PI control parameters, modulation index and delay angle the reactive power magnitude can be controlled. Due to this there is a variation in the power factor. Here it is observed that the reactive power received by the grid is increased and the power factor at grid is 0.96.

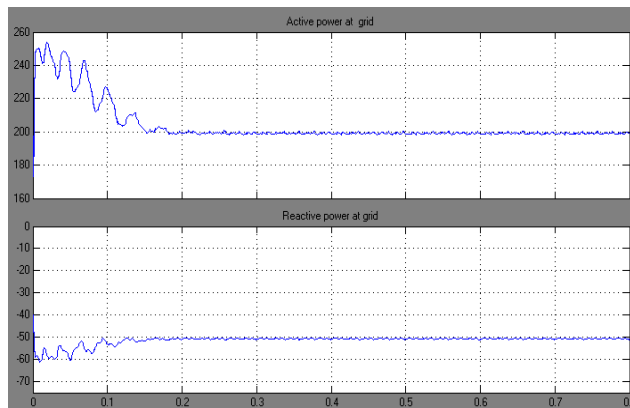


Fig. 16. Active and reactive power received by grid with control loop.

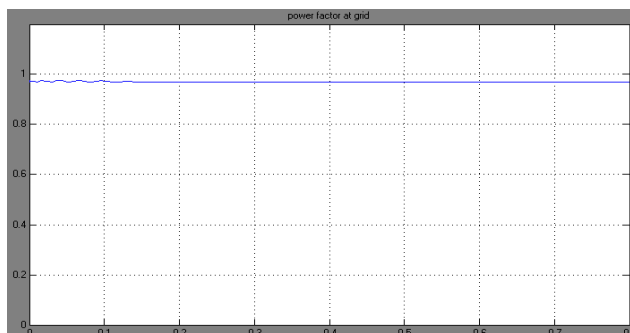


Fig. 17. Power factor at the grid with control loop.

The active and reactive power at the grid with power factor loop is as shown in Fig. 16. The active and reactive power at the grid are 200 Watts and -50 VAR respectively. The active and reactive power reaches to steady state values at 0.2 seconds. The power factor at the grid with power factor loop is as shown in Fig. 17. The p.f is 0.96. The p.f reaches to steady state at 0.2 seconds. As reactive power is decreased and having a constant active power the p.f at the grid is increased. The p.f at the grid is of more harmonics in it.

Here it can be observed that due to the power factor control loop the p.f is increased, the harmonics are reduced and it is observed that the p.f is improved from generated end to the received end. Due to this power factor loop at the rectifier unit the unity power factor is achieved at the input of the rectifier unit and hence there is no much more change in the reactive power and the active power at the grid but due to this loop the harmonics can be reduced.

The active and reactive powers at grid are 120W and -50VAR respectively.

IV. CONCLUSIONS

The modeling and simulation analysis of wind driven SEIG with power factor loop at rectifier unit, results are tested with the grid. The SEIG in its no load condition generated a phase voltage of 390 V at a speed of 1650 rpm. For a wind velocity of 6.5 m/s, the proposed inverter produced an output voltage of 390 V were obtained for grid connected SEIG driven by wind turbine. The required output voltage and active, reactive powers were obtained for a wind velocity range of 6.5m/s. From the simulation it is confirmed that as there is any variation in the excitation capacitance at a particular speed, voltage builds up faster and the magnitude of the voltage increases due to the availability of more VAR. The output voltage is controlled to give a constant voltage by

D.C/A.C link .With the use of the power factor control there is an improvement in the p.f. The ripples in the p.f are eliminated with the use of the p.f loop can be maintained to 0.96 p.f. Due to this power factor loop at the rectifier unit, maintained at unity power factor, there is no change in magnitude of the active and reactive power, which can be treated as the disadvantage. But due to power factor loop the harmonics in the active power, reactive power and power factor can be decreased up to 13th harmonic. From the FFT analysis it is also observed that PWM generates less harmonic distortion (2.55 %) in the output current and more efficient use of inverter voltage. The performance characteristics of the wind turbine SEIG are improved due to the closed loop condition and hence results in improved load performance.

V. APPENDIX

- The induction machine was three, phase 3.5kW, 415V, 7.5A, 1500r.p.m, star connected stator winding. A 3-Φ variable capacitor bank or a single capacitor was connected to the machine terminals to obtain self-excited induction generator action.

The measured machine parameters were: $r_1=11.78\Omega$; $r_2=3.78\Omega$; $L_1=L_2=10.88H$. $L_m=227.39H$

- To compute the coefficients A_4 to A_0 of equation(10), the following equations are first defined:

$$\begin{aligned}
 a &= 2\pi k(L_M r_1 + L_1 r_1 + L_2 r_1 + L_M r_2 + L r_2 + r_L L_M + r_L L_2); \\
 b &= -2 \pi N \times r_L (L_M + L_2) \\
 c &= -8\pi^3 k(LL_M r_1 + LL_2 r_1 + LL_M r_2 - r_L L_1 L_M - r_L L_2 L_M) \\
 d &= -8 \pi^3 N(r_L L_1 L_M + r_L L_2 L_1 + r_L L_2 L_M + LL_2 L_M) \\
 e &= -2\pi k r_1 r_1 r_2 \\
 g &= -4\pi^2 k(L_1 L_M + L_1 L_2 + L_2 L_M + LL_M + LL_2) \\
 h &= 4\pi^2 N(L_1 L_M + L_1 L_2 + L_2 L_M + LL_M + LL_2) \\
 i &= r_1 r_2 + r_L r_2 \\
 j &= -16\pi^4 k(LL_1 L_M + LL_2 L_M + LL_2 L_1) \\
 l &= 16\pi^4 N(LL_1 L_M + LL_1 L_2 + LL_2 L_M) \\
 m &= 4\pi^2 k(L r_1 r_2 + r_L L_M r_1 + r_L L_1 r_2 + r_L L_1 r_2 + r_L L_2 r_1 + r_L L_m r_2) \\
 p &= -4\pi^2 N r_L L_M r_1; \\
 A_4 &= cg - aj \\
 A_3 &= dg + hc + al - bj; \\
 A_2 &= eg + hd + ic - ma - bl; \\
 A_1 &= he + id - pa - bm \\
 A_0 &= ie - bp;
 \end{aligned}$$

- Air gap voltage:

The piecewise linearization of magnetization characteristic of machine is given by:

$$E_1 = 0 \quad X_m \geq 260$$

$$\begin{aligned}
 E_1 &= 1632.58 - 6.2 X_m & 233.2 \leq X_m \leq 260 \\
 E_1 &= 1314.98 - 4.8 X_m & 214.6 \leq X_m \leq 233.2 \\
 E_1 &= 1183.11 - 4.22 X_m & 206 \leq X_m \leq 214.6 \\
 E_1 &= 1120.4 - 3.9.2 X_m & 203.5 \leq X_m \leq 206 \\
 E_1 &= 557.65 - 1.144 X_m & 197.3 \leq X_m \leq 203.5 \\
 E_1 &= 320.56 - 0.578 X_m & X_m \leq 197.3
 \end{aligned}$$

REFERENCES

- Lopes, L. A. C. Almeida, and R. G "Wind-driven self-excited induction generator with voltage and frequency regulated by a reduced-rating voltage source inverter" IEEE transactions, vol. 21 , Issue 2, pp. 297 – 304, June 2006.
- Woei-Luen Chen and Yuan-Yih Hsu (September 2006). "Controller design for an induction generator driven by a variable-speed wind turbine", IEEE Transactions on Energy Conversion, vol. 21, no. 3, pp 625-635.
- Z. Chen and E. Spooner (June 2001), "Grid power quality with variable speed wind turbines," IEEE Trans. Energy Conversion, vol. 16, no. 1, pp. 148–154.
- Yaser Anagreh (2001), "Steady state performance of series DC motor powered by wind driven self-excited induction generator," *Proceedings on Rev. Energ. Ren: power Engineering*, pp.9-15.
- B. P. McGrath and D. G. Holmes (2000), "Comparison of Multi carrier PWM strategies for cascaded and Neutral Point clamped Multilevel inverter", *Proceedings on IEEE 31 St Annual Power Electronics Specialist Conference*, vol. 2, pp. 674-679.
- Rajambal and C. Chellamuthu (2002), "Modeling and simulation of grid connected wind electric generating system," *Proceedings on IEEE region conference TENCON*, vol. 3, pp.1847–1852.
- J. Rodriguez, J. S. Lai, and F. Z. Peng (August 2002), "Multilevel inverters: A survey of topologies, controls, and applications," *IEEE Trans. Industrial Electronics*, vol. 49, no. 4, pp. 724–738.
- S. Wekhande and V. Agarwal (1999), "A new variable speed constant voltage controller for self-excited induction generator with minimum control requirements," *Proceedings On Power Electronics And Drives Systems Conference*, vol. 1, pp. 98–103.



Swati Devabhaktuni received the B.Tech degree in electrical and electronics engineering from V.R.Siddhartha Engineering College, Andhra University, India in 2001, and the M.Tech degree in control systems from J.N.T.U University, in 2004. Currently, she is a Associate professor in Gokaraju rangaraju Institute of engineering and technology, Hyderabad, She is also a Research Scholer in J.N.T.U University, Hyderabad. Her research interests are the power electronics, AC motor drives , and control systems.



Dr. S. V. Jayaram Kumar received the M.E. degree in electrical engineering from the Andhra University, Vishakapatnam, India, in 1979. He received the Ph.D. degree in electrical engineering from the Indian Institute of Technology, Kanpur, in 2000. Currently, he is a professor at Jawaharlal Nehru Technological University, Hyderabad. His research interests include FACTS and Power System Dynamics, A.C drives.